CORRECTED 24 OCTOBER 2003; SEE LAST PAGE

RESEARCH ARTICLE

LMO2-Associated Clonal T Cell Proliferation in Two Patients after Gene Therapy for SCID-X1

S. Hacein-Bey-Abina,[1,2*] C. Von Kalle,[6,7,8] M. Schmidt,[6,7] M. P. McCormack,[9] N. Wulffraat,[10] P. Leboulch,[11] A. Lim,[12] C. S. Osborne,[13] R. Pawliuk,[11] E. Morillon,[2] R. Sorensen,[19] A. Forster,[9] P. Fraser,[13] J. I. Cohen,[15] G. de Saint Basile,[1] I. Alexander,[16] U. Wintergerst,[17] T. Frebourg,[18] A. Aurias,[19] D. Stoppa-Lyonnet,[20] S. Romana,[3] I. Radford-Weiss,[3] F. Gross,[2] F. Valensi,[4] E. Delabesse,[4] E. Macintyre,[4] F. Sigaux,[20] J. Soulier,[21] L. E. Leiva,[14] M. Wissler,[6,7] C. Prinz,[6,7] T. H. Rabbitts,[9] F. Le Deist,[1] A. Fischer,[1,5†‡] M. Cavazzana-Calvo[1,2†]

We have previously shown correction of X-linked severe combined immunodeficiency [SCID-X1, also known as γ chain (γc) deficiency] in 9 out of 10 patients by retrovirus-mediated γc gene transfer into autologous CD34 bone marrow cells. However, almost 3 years after gene therapy, uncontrolled exponential clonal proliferation of mature T cells (with γδ+ or αβ+ T cell receptors) has occurred in the two youngest patients. Both patients' clones showed retrovirus vector integration in proximity to the *LMO2* proto-oncogene promoter, leading to aberrant transcription and expression of *LMO2*. Thus, retrovirus vector insertion can trigger deregulated premalignant cell proliferation with unexpected frequency, most likely driven by retrovirus enhancer activity on the *LMO2* gene promoter.

Ex vivo retrovirus-mediated gene transfer into hematopoietic progenitor cells has been shown to be an efficient strategy to correct inherited diseases of the lymphohematopoietic system, provided that a strong selective advantage is conferred to transduced cells (*1*–*3*). Indeed, in 9 out of 10 patients with typical X-linked severe combined immunodeficiency [SCID-X1, or γ chain (γc) deficiency], ex vivo γc gene transfer into autologous bone marrow–derived CD34+ cells with a long terminal repeat (LTR)–driven MFG vector (*4*) resulted in the development of a functional adaptive immune system (Fig. 1A) (*2*). The clinical benefit has been so far sustained for more than 4 years in the first two treated patients; potentially, this sustained efficacy could be explained in part by the transduction of pluripotent progenitors with self-renewal capacity (*5*, *6*). The main potential risk of retrovirus-mediated gene transfer is insertional mutagenesis resulting from random retroviral integration. This could either activate proto-oncogenes over long distances (up to 100 kbp) or inactivate tumor-suppressor genes, ultimately leading to malignancies. To date, this risk has been considered very low, because it has never been observed in a clinical trial. Furthermore, only recently has evidence become available that insertion of replication-defective retrovirus vectors could contribute to malignancy in a single experimental setting (*7*). This risk assessment is now seriously challenged by our report of the occurrence of two severe adverse events in our SCID-X1 gene therapy trial.

Clinical findings. Two children (patients P4 and P5) have developed an uncontrolled clonal proliferation of mature T lymphocytes 30 and 34 months after gene therapy, respectively (*8*). These two children, 1 and 3 months old at the time of treatment, received 18×10^6 and 20×10^6 CD34(+) γc(+) cells per kg of body weight, respectively. These values are in the high range compared with those of other treated patients (range, 1.1×10^6 to 22×10^6; median, 4.3×10^6) (*1*, *2*).

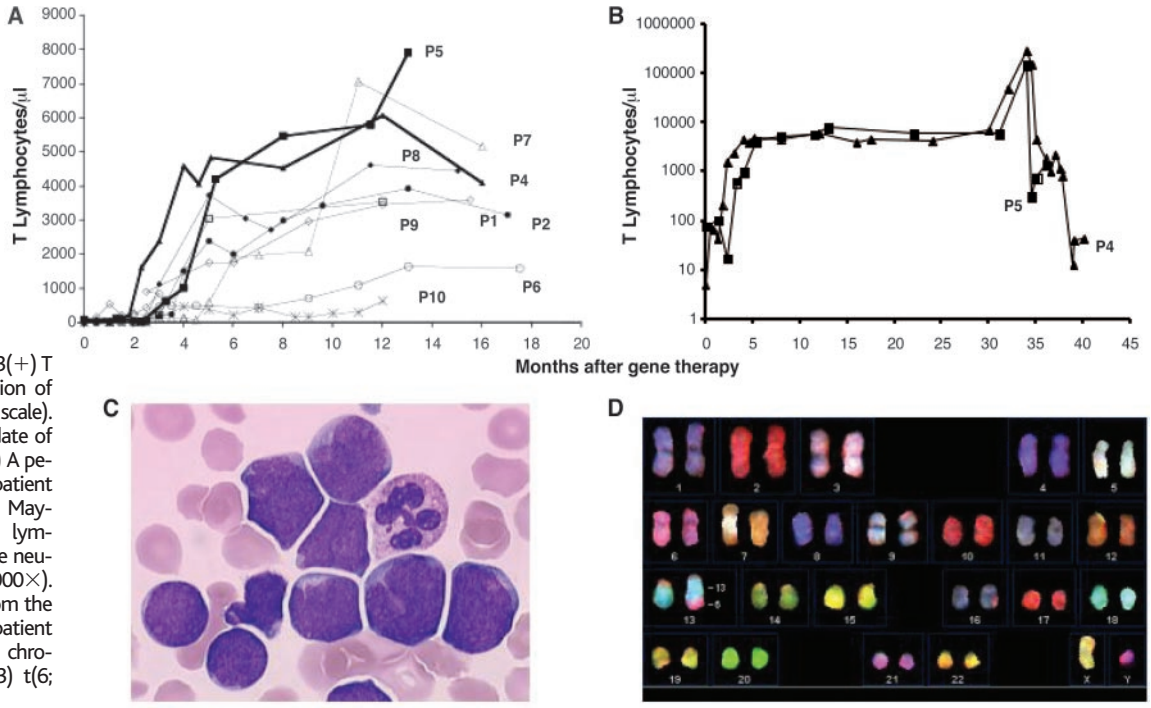

Fig. 1. Kinetics and characteristics of P4 and P5 abnormal T cells. (**A**) Longitudinal kinetics of blood T lymphocyte (CD3+) counts in treated patients (P1, P2, and P4 to P10), who recovered T cell immunity. (**B**) T cell kinetics of patients P4 (triangles) and P5 (squares), who developed an uncontrolled T lymphocyte proliferation. Absolute counts of CD3(+) T cells are shown as a function of time (on a semilogarithmic scale). Day 0 corresponds to the date of gene therapy treatment. (**C**) A peripheral blood smear from patient P4 at M+34, stained with May-Grünwald Giemsa, shows lymphoid blasts and one mature neutrophil (magnification, 1000×). (**D**) A spectral karyotype from the unstimulated blast cells of patient P4, showing the abnormal chromosome 13, derivative (13) t(6; 13) at M+34.

The total number of injected transduced cells was 30×10^6 and 25×10^6 per kg of body weight for patients P4 and P5, respectively (*2*). T cell development early after gene therapy was especially rapid and/or intense in these two patients as compared to the other treated patients (*2*) (Fig. 1A). Until months 30 and 34 after gene therapy (M+30 and M+34), respectively, patients' T cell characteristics were indistinguishable from those of age-matched controls (*2*). In patient P4, at M+30, an increase in γδ T cell counts was noticed and interpreted as the consequence of an ongoing chickenpox infection, because increases in γδ T cells have also been reported with cytomegalovirus infection (*9*). T cell counts continued to increase and fluctuated between 50,000 and 80,000 per mm^3 without any clinical signs of lymphoproliferation for 3 months (Fig. 1B). Abruptly, at M+34, T cell counts increased up to 300,000 per mm^3, with blasts noted in the blood (Fig. 1C). Concomitantly with bone marrow infiltration and detection of an enlarged spleen, these results prompted further investigation and initiation of conventional treatment for T-acute lymphoblastic leukemia (T-ALL) (*10*). A second reinduction treatment, followed by a matched unrelated bone marrow transplantation at M+40, was performed for patient P4 in the presence of a minimal residual disease. A similar T cell proliferative syndrome was detected at M+34 in patient P5 (Fig. 1B), associated with anemia, an enlarged mediastinum, and splenomegaly, although 3 months earlier, patient P5's T cell counts and immunophenotype had been normal. Treatment of patient P5 was initiated under the Children's Cancer Study Group T-ALL protocol. Complete clinical remission was achieved within 2 months and has been sustained, although a small number of abnormal cells persist in patient P4 at M+45. Both patients are currently alive and well.

Clonality of T cell proliferations. One monoclonal T cell receptor (TCR) γδ T cell clone (Vγ9Vδ1) was identified in the peripheral blood of patient P4 by quantitative immunoscope analysis (*11*–*14*) and confirmed by TCR sequencing. These T cells were phenotypically mature and did not express antigens that belong to other hematopoietic lineages (*15*). γc expression was detectable on the cell surface within the normal intensity range for mature T cells. At the time of clinical manifestations, a partial trisomy 6 with a t(6; 13) chromosome translocation was detected in the P4 clone (Fig. 1D). At the time of the diagnosis, three different TCR αβ T cell clones (Vβ1, Vβ2, and Vβ23) were identified in the peripheral blood of patient P5. These cells had a mature phenotype and expressed γc at the cell surface. Two chromosomal aberrations were detected in P5 clones, a unique SIL-TAL1 fusion transcript and a trisomy 10. Thus, in both cases, clinical disease was related to the uncontrolled proliferation of mature T cells with leukemia-like characteristics.

Absence of replication-competent retroviruses. The presence of replication-competent retroviruses could have favored the occurrence of multiple integrations leading to oncogenic events (*16*, *17*). This hypothesis was excluded in both cases by functional as well as direct detection assays. Thus, the β galactosidase mobilization test performed on a Mus Dunni (*18*) cell line was found repeatedly negative with P4 and P5 serum samples from M+3 up to M+34. Amphotropic envelope and reverse transcriptase and integrase genes were not found by Southern hy-

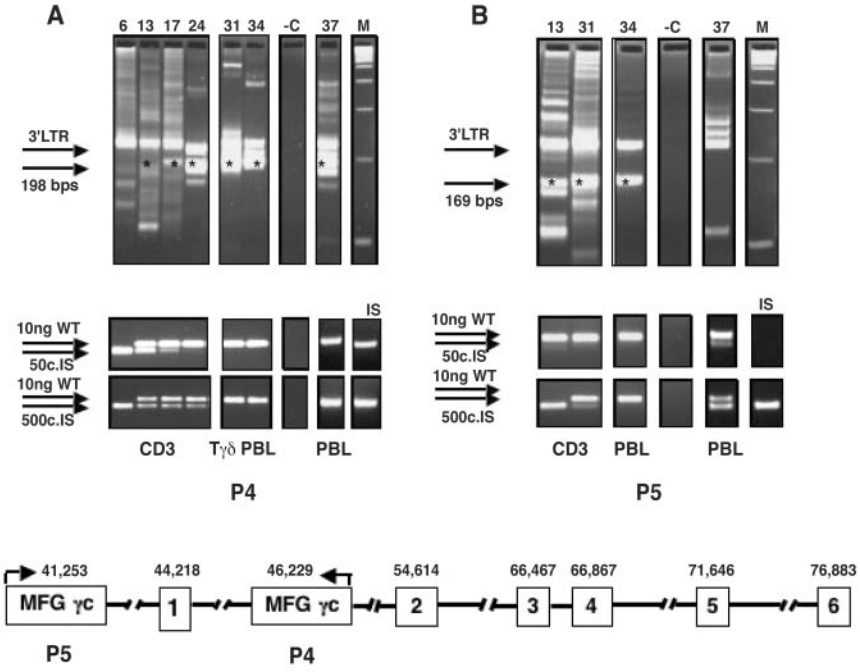

Fig. 2. Clonal proliferations associated with provirus integration into the LMO2 locus. (**A** and **B**) LAM integration site analysis and quantification of the lymphoproliferative T cell clones in patients (A) P4 and (B) P5. LAM-PCR (upper panels) was performed on 5 to 20 ng of DNA from sorted CD3+ T cells (CD3), Tγδ T cells, or peripheral blood leukocytes (PBL), by linear LTR primer extension, second-strand synthesis, restriction digest, cassette ligation, and exponential amplification (*14*), at different time points after treatment. Clonal insertion-site amplification products [P4: 198 base pairs (bp), P5: 169 bp] and an internal vector 3′ LTR amplification product were sequenced at the time of lymphoproliferation (M+34, in both cases). Time-course analysis indicates a conversion of clonal composition from polyclonal to monoclonal. For QC PCR detection, amplification of 10 ng of patient wild-type (WT) DNA from sorted CD3, Tγδ, or PBL cells was performed with primers to detect the lymphoproliferation clones (*14*). To estimate the contribution in each patient of the lymphoproliferative clones to gene-modified lymphopoiesis, the specific 5′ insertion-site fusion sequences were coamplified in competition with a defined copy number of a 26-bp internally deleted standard (IS) DNA template (addition of 50 copies or 500 copies). Time-course analysis revealed a progressive clonal growth of the lymphoproliferative clone, starting at least 13 months after the reinfusion of gene-modified cells in both patients analyzed. Numbers along the top denote months after transplantation. Nontransduced human leukocyte DNA (0.2 to 1.0 μg) was used as a negative control (−C). Asterisks denote clonal bands with their identity confirmed by sequencing. M, 100-bp ladder; c., copies. (**C**) *LMO2* gene map of activating retrovirus vector insertions. Loci of retroviral insertion in P4 and P5 clones were characterized by LAM PCR sequencing of the 5′ insertion-site fusion sequence (*14*). Sequence mapping to the human genomic database indicated a 100% match to the 5′ *LMO2* genomic DNA locus on chromosome 11 (clone RP1-22J9, NCBI accession no. NM_005574).The first nucleotide of each exon is also indicated.

[1]INSERM Unit 429, [2]Department de Biotherapie Assistance Publique–Hopitaux de Paris, [3]Laboratoire de Cytogénétique, [4]Laboratoire Central d'Hématologie and CNRS Unité de Recherche Associée 1461, Université Paris V, [5]Unité d'Immunologie et d'Hématologie Pédiatriques, Hôpital Necker, 75743 Paris, Cedex 15, France. [6]Department of Internal Medicine, [7]Institute of Molecular Medicine and Cell Research, University of Freiburg, Freiburg, Germany. [8]Children's Hospital Research Foundation, Cincinnati, OH, USA. [9]Medical Research Council, Laboratory of Molecular Biology, Hills Road, Cambridge CB2 2QH, UK. [10]University Medical Center Utrecht–Wilhelmina Kinderziekenhuis, Utrecht, Netherlands. [11]Harvard Medical School and Genetics Division, Brigham and Women's Hospital, Boston, MA 02115, USA. [12]INSERM Unit 277, Institut Pasteur, 75730 Paris, France. [13]Laboratory of Chromatin and Gene Expression, Developmental Genetics Programme, The Babraham Institute, Cambridge CB2 4AT, UK. [14]Department of Pediatrics, Louisiana State University Health Sciences Center and Children's Hospital, New Orleans, LA 70112, USA [15]Medical Virology Section, Laboratory of Clinical Investigation, National Institute of Allergy and Infectious Diseases, Bethesda, MD 20892, USA. [16]The Children's Hospital at Westmead, Sydney, NSW 2145, Australia. [17]University and Children's Hospital, Lindwurmstraβe 4, 80337 Munich, Germany. [18]Service de Genetique, Centre Hospitalo-Universitaire et Equipte Mixte INSERM 9906, Faculté de Médecine et de Pharmacie, 76183 Rouen, France. [19]INSERM Unit 434, [20]Department of Oncology Genetics, Institut Curie, Paris, Cedex 15, France. [21]INSERM Unit 462, Hôpital Saint Louis, Paris, France.

*These authors contributed equally to this work.
†These authors contributed equally to this work.
‡To whom correspondence should be addressed. E-mail: fischer@necker.fr

bridization in γδ or αβ clonal cell populations from either patient (fig. S1, A and B). The potential presence of VL30 murine retrotransposons, known to be present in murine leukemia virus particles produced by a number of murine packaging cell lines including ψCRIP and recently found to be associated with metastatic melanoma (*19*), was also excluded by Southern hybridization analysis (fig. S1C).

Insertional mutagenesis of the *LMO2* locus. Insertional mutagenesis directly induced by retrovirus insertion was an obvious alternative potential mechanism. Multiple integration sites (≥50) with one integration site per cell were detected in the patients' peripheral T cells before the onset of cell proliferation, through linear amplification–mediated polymerase chain reaction (LAM-PCR) (Fig. 2, A and B) (*14*). In contrast, T cell clones at the time of lymphoproliferation exhibited a single insertion site in both cases. These insertions became progressively predominant over time in patient P4, as shown by quantitative competitive (QC) PCR analysis (Fig. 2A) (*14*). In the Vγ9Vδ1 P4 clone, the single copy of the retrovirus vector was mapped to the short arm of chromosome 11, close to the distal (hematopoietic) promoter of the *LMO2* locus (Fig. 2C). It was found inserted at position 46,229 (the first nucleotide of exon 1 is 44,218), within the first intron in reverse orientation. Sorted populations of the different T cell clones from patient P5 (i.e., Vβ1, Vβ2, and Vβ23) possessed a unique integration site also located in the *LMO2* locus, at position 41,253, 3 kbp upstream of the first *LMO2* exon in forward orientation (Fig. 2C). [Sequences were aligned to the human genome sequence with BLASTN from the National Center for Biotechnology Information (NCBI) and the Blat database from the University of California, Santa Cruz.] LMO2 (LIM domain only–2) is a cysteine-rich *Lin*-11 *Isl*-1 *Mec*-3 (LIM) finger protein required for normal hematopoiesis (*20*–*22*). Because complete LMO2 deficiency fails to contribute to any stage of embryonic or adult hematopoiesis in chimeric *Lmo2*$^{-/-}$ mice (*22*), this transcription factor is considered a central regulator of hematopoiesis (*23*–*26*).

To investigate the effect of the retroviral integration sites on transcription of *LMO2*, we analyzed the expression of the gene and the integrity of the proviral transcripts in the T cell clones. *LMO2* transcripts of the expected 3.3-kb size were detected by Northern blot analysis in clones from both patients, contrasting with the absence of detection in control TCR γδ+ or αβ+ T cells. Quantitative reverse transcription (RT)–PCR, as well as Northern blot analysis, revealed levels of transcript equivalent to those in a positive-control mouse erythroleukemia (MEL) cell line in both γδ and αβ clones. To determine whether the presence of the MFG γc provirus influenced the splicing of the first intron of the *LMO2* transcript, we performed exon-specific RT-PCR. Sequence analysis of the amplified fragment showed the expected exon 1/2 junction as compared to normal control *LMO2* messenger RNA (mRNA) (fig. S2). In T cell clones from both patients, normally migrating LMO2 protein was abundantly detected by Western blotting (Fig. 3A) at a level of expression comparable to levels of MEL and transfected Chinese hamster ovary (CHO) cells (*14*). RNA fluorescence in situ hybridization (FISH) analysis, using probes specific for *LMO2* and γc, showed colocalization of the two messages, indicating that it was indeed the retrovirus-targeted *LMO2* allele that was transcribed in both cases (Fig. 3B) (*14*). Moreover, we took advantage of a single-nucleotide polymorphism (SNP) between the two *LMO2* alleles in exon 1 of patient P4 to confirm which allele was expressed. Long-range PCR was performed on genomic DNA from P4 blasts, with a forward primer located upstream of the *LMO2* exon 1 SNP and a reverse primer at the beginning of the provirus sequence, and produced the expected 2.1-kbp band. Cloning and sequencing of the amplified 2.1-kbp fragment confirmed that the exon 1 SNP matched the one detected in the *LMO2* mRNA. These data are consistent with retroviral cis-activation that results in monoallelic *LMO2* expression in both cases. The aberrant expression of *LMO2* is thus a hallmark of proliferating clones found in both patients, and it appears to be directly involved as a primary cause of the cellular transformation. Given the integration site and integrity of the *LMO2* transcripts, these data strongly suggest that the viral LTR exerts an enhancer activity on the distal (hematopoietic) *LMO2* promoter in these cases. However, the disruption of silencing or of putative silencer(s) by the retrovirus integrations has not been formally excluded. This interpretation is consistent with the observation that aberrant *LMO2* expression is triggered by the chromosomal translocation t(11; 14)(p13; p11) (*20*, *27*) and by the less common variant translocation t(7; 11)(q35; P13) in T-ALL. In addition, *Lmo2* transgenic mice were shown to develop T-ALL (*28*) within 10 months, despite the fact that the transgene expression was not restricted to T cells (*29*–*32*).

Kinetics of clonal expansion. Using both the immunoscope technique and a clonotypic quantitative analysis (*14*), we were able to trace abnormal clones back in time. The growth kinetics of these clones were further confirmed by QC PCR (*14*). Results from these analyses consistently showed that the abnormal LMO2(+) Vγ9Vδ1 T cell clone populations found in patient P4 became detectable from M+13, then experienced continuous exponential growth up to M+34 (Figs. 2A and 4, A and B). Equivalent results

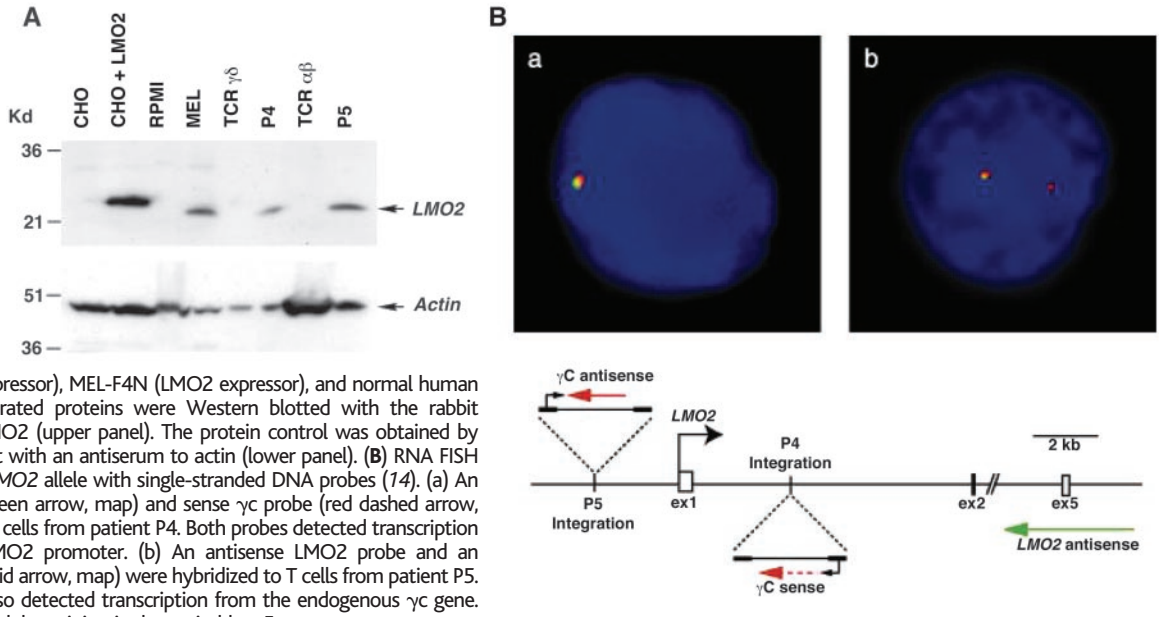

Fig. 3. LMO2 expression in clonal T cells. (**A**) Detection of LMO2 protein in clonal T cells. Whole cell protein extracts were made from 5 × 10^5 clonal cells from patients P4 and P5 for Western blot analysis (*14*). As controls, proteins were made from 1 × 10^5 CHO cells or CHO cells transfected with pEF-BOS-LMO2-myc or from 5 × 10^5 RPMI-8402 (LMO2 nonexpressor), MEL-F4N (LMO2 expressor), and normal human Tγδ and Tαβ cells. Separated proteins were Western blotted with the rabbit polyclonal antibody to LMO2 (upper panel). The protein control was obtained by reprobing the stripped blot with an antiserum to actin (lower panel). (**B**) RNA FISH analysis of the activated *LMO2* allele with single-stranded DNA probes (*14*). (a) An antisense LMO2 probe (green arrow, map) and sense γc probe (red dashed arrow, map) were hybridized to T cells from patient P4. Both probes detected transcription that originated at the LMO2 promoter. (b) An antisense LMO2 probe and an antisense γc probe (red solid arrow, map) were hybridized to T cells from patient P5. The antisense γc probe also detected transcription from the endogenous γc gene. 4′-6-diamidino-2-phenylindole staining is shown in blue. Ex., exon.

obtained by both methods of detection suggested that no other LMO2(+) T cell clone was present. Although samples from patient P5 were fewer, abnormal clones could be detected at low frequencies 3 months before overt disease (Figs. 2B and 4C). Together, overall growth kinetics showed a rather similar pattern. Disease phenotype was similar in both cases to that seen in *Lmo2* transgenic mice (*30*). This strongly suggests that additional factors leading to secondary genomic alterations were required for the development of the leukemia-like stage of lymphoproliferation in these patients.

Potential cofactors. Signaling mediated through the γc-cytokine receptor subunit is likely responsible for the selective advantage of transduced over nontransduced cells, by mediating proliferative and survival signals (*33*, *34*). Potentially, therefore, an aberrant γc-mediated signal might also be a contributing factor in this leukemia-like disease. However, no overexpression of the common γ chain in patients' clones was observed. Gain-of-function mutations of the γc receptor subunit could lead to sustained activation of the specifically associated tyrosine kinase JAK3, thus contributing to the monoclonal proliferation. To exclude this hypothesis, we entirely sequenced the integrated provirus and found it to be nonmutated, including the γc complementary DNA (cDNA). To further rule out an abnormal, triggered clonal activation through γc, we analyzed the in vivo phosphorylation status of JAK3 (*14*). No constitutive activation of JAK3 in patients' clones could be detected, although this pathway could be activated in vitro by interleukin (IL)–7 or IL-15 (Fig. 5). However, these results do not rule out a role for the γc transgene in association with overexpression of *LMO2* as a potential synergistic factor for driving the proliferation of precursors or mature T cells. This hypothesis will require further testing in a relevant animal model.

A role for secondary events, such as the chickenpox infection that occurred at M+30 in patient P4, in providing a synergistic influence is also conceivable, as the varicella zoster virus (VZV) genome was detected in the P4 T cell clone (*35*). VZV infection could also have triggered a transient immunosuppression that might have favored the emergence of the abnormal clone. Alternatively, the Vγ9Vδ1 T cell clone could have been amplified in the context of the antiviral immune response toward VZV. However, no such infection was detected in the course of patient P5's disease. In an alternative scenario, the possible influence of a genetic predisposition factor in the family of patient P4 might have contributed, because the patient's sister and a third-degree cousin developed medulloblastoma in childhood. Although we do not completely exclude this as a possibility, a search for mutations in the *TP53*, *ATM*, *MLH1*, and *MSH2* genes was negative and no loss of heterozygosity was evident from comparative genomic hybridization-array analysis (*36*). No such familial predisposition was present in the family of patient P5. Finally, given the recent description of a significant incidence of leukemia-associated rearrangements present in normal cord blood samples (*37*), one may speculate that if such cells were targeted by retroviral insertion, they might obtain a proliferative advantage.

Scenario for clonal proliferation. Taken together, our data suggest that the following scenario might account for occurrence of the lym-

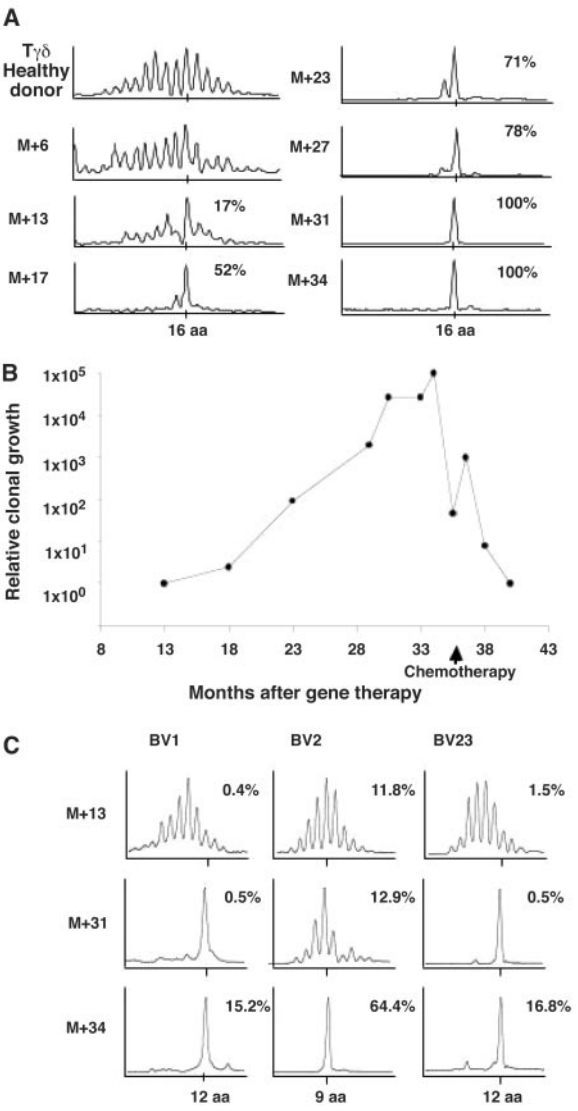

Fig. 4. Kinetics of abnormal clone growth. (**A**). Longitudinal immunoscope study of Vδ1 T lymphocytes from patient P4. cDNA prepared from the peripheral blood was amplified with Vδ1/Cδ–specific primers (*14*). PCR products were then subjected to run-off reactions with a nested fluorescent primer specific to the Cδ segment. The fluorescent products were separated and analyzed on a 373A sequencer (Applied Biosystems). The size and intensity of each band were analyzed with the Immunoscope software. On the *y* axis, the fluorescent intensity is plotted in arbitrary units; the *x* axis represents the different lengths of CDR3 in amino acids. Although a Gaussian distribution of different CDR3 lengths is characteristic of normal Vδ repertoire (upper left panel), proliferating cells can be detected as a deviation from the Gaussian distribution visible as early as M+13. Percentages indicate the frequency of the proliferative clone among Tδ1 cells (CDR3 16 amino acid residues). This frequency was obtained in quantitative amplification experiments, with a clonotypic specific primer and a Vδ1 TaqMan probe characteristic of the unique Vδ1/Jδ1 sequence observed at M+31 (*14*). aa, amino acid. (**B**) Semiquantitative estimation of P4 clone frequency as based on QC PCR analysis of the integration site (Fig. 2A) and immunofluorescence analysis with an antibody to Vδ1. (**C**) Longitudinal immunoscope study of Vβ T lymphocytes from patient P5. cDNA prepared from the peripheral blood was amplified with each of 24 TCR variable region of the β chain (TCRBV) family–specific primers together with a TCR constant region (TCRBC) primer and a Minor groove binder–TaqMan probe for TCRBC (*14*). Real-time quantitative PCR was carried out in a ABI5700 system (Applied Biosystems). PCR products were then subjected to run-off reactions with a nested fluorescent primer specific to the Cβ segment. The fluorescent products were separated and analyzed on a 373A sequencer. The size and intensity of each band were analyzed with the Immunoscope software. CDR3 length distributions obtained with the BV1, BV2, and BV23 primers are displayed. Percentage indicates the usage of BV, as derived from quantitative amplification. The loss of the polyclonality is less evident at M+31 in the BV2 family than in the BV1 and BV23 families, because of its higher expression level.

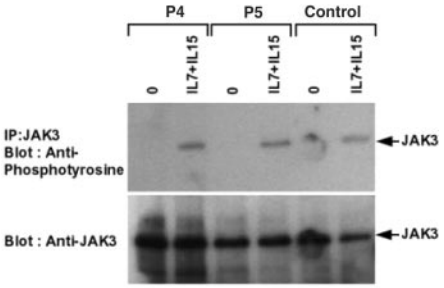

Fig. 5. The tyrosine phosphorylation status of Jak3 in P4 and P5 T cell clones. T cells were stimulated for 15 min with IL-7 (20 ng/ml) and IL-15 (20 ng/ml) or were not stimulated (0, resting cells). Lysates were then immunoprecipitated (IP) with an antibody to Jak3 and immunoblotted with an antibody to phosphotyrosine (upper panel). The blot was then stripped and reprobed with an antibody to Jak3 (lower panel) (*14*).

phocyte proliferations observed in these patients. *LMO2* targeting suggests either that there is a "physical hotspot" of integration at this locus, or more likely, that random, activating, *LMO2* integrants are selected simply by the growth advantage conferred on them. The chance of integration of any active gene is assumed to be $\sim 1 \times 10^{-5}$ (a rough estimate of a random hit within 10 kbp among the estimated transcriptionally active 1×10^9 base pairs. It is likely that each patient received at least 1 to 10 *LMO2*-targeted cells, because the patients received 1×10^6 or more transduced T lymphocyte precursors (estimating that at least 1% of the total number of injected transduced cells—92×10^6 and 133×10^6 for patients P4 and P5, respectively—could give rise to T cells). It will be crucial to understand the site distribution and mechanism of retroviral integration in human CD34 cells in order to more accurately assess this risk. The availability of the human genome sequence makes this work feasible (*38*, *39*). It is tempting to speculate that SCID-X1–related features may have contributed to the unexpectedly high rate of leukemia-like syndrome. Indeed, it is possible that, because of the differentiation block, there are more T lymphocyte precursors among CD34 cells in SCID-X1 marrow than in marrow of normal controls, thus augmenting the number of cells at risk for vector integration and further proliferation once the γc transgene is expressed. The massive capacity of T cell precursors to become amplified in an "empty compartment" is another possible factor that favors the development of disease (*40*). Finally, patients P4 and P5 were the youngest in our study. Given the exceptional proliferative capacity of neonatal hematopoiesis, young age per se could also increase the number of precursor cells at risk for insertional mutagenesis. These hypotheses can now be tested by the design of predictive model(s) that enable assessment of the safety of modified gene therapy strategies that should be envisaged to treat SCID-X1 patients, as justified by the efficacy of gene therapy observed in this trial. Our observations demonstrate that the safety profile of each gene transfer strategy needs to be addressed individually for each disease in relation to its pathophysiology and the functions of the transgene product.

References and Notes

1. M. Cavazzana-Calvo *et al.*, *Science* **288**, 669 (2000).
2. S. Hacein-Bey-Abina *et al.*, *N. Engl. J. Med.* **346**, 1185 (2002).
3. A. Aiuti *et al.*, *Science* **296**, 2410 (2002).
4. S. Hacein-Bey *et al.*, *Blood* **87**, 3108 (1996).
5. M. Schmidt *et al.*, *Blood* **100**, 2737 (2002).
6. M. Schmidt *et al.*, in preparation.
7. Z. Li *et al.*, *Science* **296**, 497 (2002).
8. S. Hacein-Bey-Abina *et al.*, *N. Engl. J. Med.* **348**, 255 (2003).
9. X. Lafarge *et al.*, *J. Infect. Dis.* **184**, 533 (2001).
10. W. A. Kamps *et al.*, *Blood* **94**, 1226 (1999).
11. C. Pannetier *et al.*, *Proc. Natl. Acad. Sci. U.S.A.* **90**, 4319 (1993).
12. J. Dechanet *et al.*, *J. Clin. Invest.* **103**, 1437 (1999).
13. A. Lim *et al.*, *J. Immunol. Methods* **261**, 177 (2002).
14. Materials and methods are available as supporting material on *Science* Online.
15. Immunofluorescence study revealed that P4 and P5 blast cells were positive for CD3, CD7, CD5, CD28, CD45RO, γc, and CD8 (for P5) and negative for CD4, CD1, CD10, CD34, CD19, CD56, and CD14.
16. R. E. Donahue *et al.*, *J. Exp. Med.* **176**, 1125 (1992).
17. E. F. Vanin, M. Kaloss, C. Broscius, A. W. Nienhuis, *J. Virol.* **68**, 4241 (1994).
18. M. Printz *et al.*, *Gene Ther.* **2**, 143 (1995).
19. X. Song *et al.*, *Proc. Natl. Acad. Sci. U.S.A.* **99**, 6269 (2002).
20. T. Boehm, L. Foroni, Y. Kaneko, M. F. Perutz, T. H. Rabbitts, *Proc. Natl. Acad. Sci. U.S.A.* **88**, 4367 (1991).
21. A. J. Warren *et al.*, *Cell* **78**, 45 (1994).
22. Y. Yamada *et al.*, *Proc. Natl. Acad. Sci. U.S.A.* **95**, 3890 (1998).
23. T. H. Rabbitts, *Oncogene* **20**, 5763 (2001).
24. V. E. Valge-Archer *et al.*, *Proc. Natl. Acad. Sci. U.S.A.* **91**, 8617 (1994).
25. I. Wadman *et al.*, *EMBO J.* **13**, 4831 (1994).
26. I. A. Wadman *et al.*, *EMBO J.* **16**, 3145 (1997).
27. B. Royer-Pokora, U. Loos, W. D. Ludwig, *Oncogene* **6**, 1887 (1991).
28. I. S. Garcia *et al.*, *Oncogene* **6**, 577 (1991).
29. P. Fisch *et al.*, *Oncogene* **7**, 2389 (1992).
30. R. C. Larson *et al.*, *Oncogene* **9**, 3675 (1994).
31. G. A. Neale, J. E. Rehg, R. M. Goorha, *Blood* **86**, 3060 (1995).
32. G. A. Neale, J. E. Rehg, R. M. Goorha, *Leukemia* **11**, 289 (1997).
33. K. Sugamura *et al.*, *Adv. Immunol.* **59**, 225 (1995).
34. O. Lantz, I. Grandjean, P. Matzinger, J. P. Di Santo, *Nature Immunol.* **1**, 54 (2000).
35. J. I. Cohen, unpublished data.
36. A. Aurias, unpublished data.
37. H. Mori *et al.*, *Proc. Natl. Acad. Sci. U.S.A.* **99**, 8242 (2002).
38. A. R. Schroder *et al.*, *Cell* **110**, 521 (2002).
39. X. Wu, Y. Li, B. Crise, S. M. Burgess, *Science* **300**, 1749 (2003).
40. A. A. Freitas, B. Rocha, *Annu. Rev. Immunol.* **18**, 83 (2000).

41. We are indebted to the families of the patients for their continuous support; to the medical and nursing staff of the Unité d'Immunologie et d'Hématologie Pédiatriques, Hôpital des Enfants Malades, for patient care; to F. Calvo, A. O. Cavazzana, D. Papadopoulo, P. Kourilsky, H. Bruzzoni-Giovanelli, C. Thibaut, P. Kastner, M. Bonneville, H. Vié, E. Vivier, and P. Paule for their contribution to the study; and to C. Hue for technical help. Supported by grants from INSERM; the Bundesministerium für Bildung, Wissenschaft, Forschung und Technologie; Deutsche Forschung Gemeinschaft; the Association Française contre les Myopathies; the Programme Hospitalier de Recherche Clinique of the Health Ministry (France); Assistance Publique–Hôpitaux de Paris; European Community contract no. QLK3-CT 2001 (G. Wagemaker, coordinator); and the Jeffrey Modell Foundation.

Supporting Online Material

www.sciencemag.org/cgi/content/full/302/5644/415/DC1
Materials and Methods
Figs. S1 and S2
References and Notes

27 June 2003; accepted 4 September 2003

REPORTS

A Hybridization Model for the Plasmon Response of Complex Nanostructures

E. Prodan,[1] C. Radloff,[2] N. J. Halas,[2,3]* P. Nordlander[1,3]

We present a simple and intuitive picture, an electromagnetic analog of molecular orbital theory, that describes the plasmon response of complex nanostructures of arbitrary shape. Our model can be understood as the interaction or "hybridization" of elementary plasmons supported by nanostructures of elementary geometries. As an example, the approach is applied to the important case of a four-layer concentric nanoshell, where the hybridization of the plasmons of the inner and outer nanoshells determines the resonant frequencies of the multilayer nanostructure.

The fabrication of materials on a nanoscale can be used to enhance and exploit properties that become stronger under conditions of reduced dimensionality. In metallic systems, the conduction electron charge density and its corresponding electromagnetic field can undergo plasmon oscillations. Because of the nature of the optical constants for noble metals, the charge oscillations can propagate along the surface (rather than vanish evanescently) at optical frequencies. These surface plasmons can be excited by incident light in a process that depends on the dielectric constant of the material at the metal's surface, an effect that is exploited in surface plasmon resonance spectroscopy. In particles of dimensions on the order ofthe plasmon resonance wavelength, this surface plasmon dominates the electromagnetic response of the structure.

Recent advancements in the chemical synthesis of metal nanostructures have led to a proliferation of various shapes such as

[1]Department of Physics, [2]Department of Chemistry, [3]Department of Electrical and Computer Engineering, and the Rice Quantum Institute, Rice University, Houston, TX 77251, USA.

*To whom correspondence should be addressed. E-mail: halas@rice.edu

ERRATUM

post date 24 October 2003

RESEARCH ARTICLES: "LMO2-associated clonal T cell proliferation in two patients after gene therapy for SCID-X1" by S. Hacein-Bey-Abina *et al.* (17 Oct. 2003, p. 415). The second and third authors, C. Von Kalle and M. Schmidt, should have had asterisks after their names, to indicate shared first authorship with S. Hacein-Bey-Abina. The asterisks were inadvertently omitted because of an editorial error.